Genes & Diseases (2024) 11, 1009–1021

Available online at www.sciencedirect.com

ScienceDirect

journal homepage: www.keaipublishing.com/en/journals/genes-diseases

FULL LENGTH ARTICLE

Vitamin D-binding protein in plasma microglia-derived extracellular vesicles as a potential biomarker for major depressive disorder

Gaojia Zhang [a,1], Ling Li [a,1], Yan Kong [b,1,**], Dandan Xu [a], Yu Bao [c], Zhiting Zhang [d], Zhixiang Liao [e], Jiao Jiao [a], Dandan Fan [a], Xiaojing Long [e], Ji Dai [d,f], Chunming Xie [a], Zhiqiang Meng [c,d,f,***], Zhijun Zhang [a,g,*]

[a] *Department of Neurology, Affiliated Zhongda Hospital, Research Institution of Neuropsychiatry, School of Medicine, Southeast University, Nanjing, Jiangsu 210009, China*
[b] *Department of Biochemistry and Molecular Biology, School of Medicine, Southeast University, Nanjing, Jiangsu 210009, China*
[c] *Shenzhen Key Laboratory of Drug Addiction, Brain Cognition and Brain Disease Institute, Shenzhen Institute of Advanced Technology, Chinese Academy of Sciences (CAS), Shenzhen, Guangdong 518000, China*
[d] *CAS Key Laboratory of Brain Connectome and Manipulation, The Brain Cognition and Brain Disease Institute (BCBDI), Shenzhen Institute of Advanced Technology, Chinese Academy of Sciences, Shenzhen, Guangdong 518055, China*
[e] *Lauterbur Research Center for Biomedical Imaging, Shenzhen Institute of Advanced Technology, Chinese Academy of Sciences, Shenzhen, Guangdong 518055, China*
[f] *Shenzhen-Hong Kong Institute of Brain Sciences-Shenzhen Fundamental Research Institutions, Shenzhen, Guangdong 518000, China*

* Corresponding author. Department of Neurology, Affiliated Zhongda Hospital, Research Institution of Neuropsychiatry, School of Medicine, Southeast University, Nanjing, Jiangsu 210009, China; Brain Cognition and Brain Disease Institute, Shenzhen Institute of Advanced Technology, Chinese Academy of Sciences, Shenzhen, Guangdong 518055, China.
** Corresponding author. Department of Biochemistry and Molecular Biology, School of Medicine, Southeast University, Nanjing, Jiangsu 210009, China.
*** Corresponding author. Shenzhen Key Laboratory of Drug Addiction, Brain Cognition and Brain Disease Institute (BCBDI), Shenzhen Institute of Advanced Technology, Chinese Academy of Sciences (CAS); CAS Key Laboratory of Brain Connectome and Manipulation, the BCBDI, Shenzhen Institute of Advanced Technology, CAS; Shenzhen-Hong Kong Institute of Brain Sciences-Shenzhen Fundamental Research Institutions, Shenzhen, Guangdong 518000, China.
E-mail addresses: kongyancn@163.com (Y. Kong), zhiqiang-meng@163.com (Z. Meng), janemengzhang@vip.163.com (Z. Zhang).
Peer review under responsibility of Chongqing Medical University.

https://doi.org/10.1016/j.gendis.2023.02.049

[g] *Brain Cognition and Brain Disease Institute, Department of Mental Health and Public Health, Faculty of Life and Health Sciences, Shenzhen Institute of Advanced Technology, Chinese Academy of Sciences, Shenzhen, Guangdong 518055, China*

Received 11 November 2022; accepted 21 February 2023
Available online 10 April 2023

KEYWORDS
Biomarker;
Cerebrospinal fluid;
Major depressive disorder;
Microglia derived extracellular vesicles;
Vitamin-D binding protein

Abstract No well-established biomarkers are available for the clinical diagnosis of major depressive disorder (MDD). Vitamin D-binding protein (VDBP) is altered in plasma and postmortem dorsolateral prefrontal cortex (DLPFC) tissues of MDD patients. Thereby, the role of VDBP as a potential biomarker of MDD diagnosis was further assessed. Total extracellular vesicles (EVs) and brain cell-derived EVs (BCDEVs) were isolated from the plasma of first-episode drug-naïve or drug-free MDD patients and well-matched healthy controls (HCs) in discovery (20 MDD patients and 20 HCs) and validation cohorts (88 MDD patients and 38 HCs). VDBP level in the cerebrospinal fluid (CSF) from chronic glucocorticoid-induced depressed rhesus macaques or prelimbic cortex from lipopolysaccharide (LPS)-induced depressed mice and wild control groups was measured to evaluate its relationship with VDBP in plasma microglia-derived extracellular vesicles (MDEVs). VDBP was significantly decreased in MDD plasma MDEVs compared to HCs, and negatively correlated with HAMD-24 score with the highest diagnostic accuracy among BCDEVs. VDBP in plasma MDEVs was decreased both in depressed rhesus macaques and mice. A positive correlation of VDBP in MDEVs with that in CSF was detected in depressed rhesus macaques. VDBP levels in prelimbic cortex microglia were negatively correlated with those in plasma MDEVs in depressed mice. The main results suggested that VDBP in plasma MDEVs might serve as a prospective candidate biomarker for MDD diagnosis.

Introduction

Major depressive disorder (MDD) is the most common severe mental illness, ranking second in the total burden of human diseases.[1] COVID-19 pandemic further increases the prevalence and the burden of MDD.[2,3] However, so far, its diagnosis still depends on clinical manifestations, since reliable biomarkers for clinical diagnosis are still under investigation.[4,5] The screening of candidate molecules based on multi-source biological samples from clinical patients and model animals has recently been in full swing[5–9] thanks to the rapid development of technologies of multi-omics and bioinformatics.[10] Nevertheless, it is extremely difficult to obtain samples from biopsy or autopsy of the brain tissues even cerebrospinal fluid (CSF) from depressed patients.[11] Moreover, a recent systematic review and meta-analysis further showed that the levels of candidate biomarkers in the peripheral blood are not remarkably correlated with those in the brain tissue or CSF,[12] suggesting that most biomarkers measured in the peripheral blood cannot directly represent the situation in the central nervous system (CNS). Therefore, it is of utmost importance to successfully isolate and characterize candidate molecules from peripheral blood that can represent CNS.[13]

Extracellular vesicles (EVs), including exosomes and ectosomes (microvesicles), are small membranous vesicles budding directly from the cell surface, thus being released from the cell membrane into the extracellular environment and normally found in various body fluids.[14] They contain a variety of biomolecules from the cell they originated, which are packaged and transported to target cells in different tissues.[14,15] They even cross the blood–brain barrier (BBB) for central and peripheral communication.[16] The continuous breakthrough and establishment of technologies for the isolation and characterization of EVs[17–19] have allowed the identification of candidate molecules in plasma exosomes derived from different brain cells, such as neurons,[20–22] oligodendrocytes,[23] astrocytes,[17] and microglia.[19] These molecules directly reflect their levels in CNS, representing the promising technology to determine biomarkers of brain diseases from peripheral blood. This technique has just been established and applied to diagnosis, differential diagnosis, and the assessment of the treatment response in patients with Alzheimer's disease (AD),[24–27] Parkinson's disease (PD),[22,28–32] multiple system atrophy (MSA),[23,28] Down syndrome,[33] and traumatic brain injury.[34–36] Importantly, some recently published articles evaluate potential biomarkers in neuron-derived EVs (NDEVs) or astrocyte-derived EVs (ADEVs) enriched from plasma or serum of MDD patients, for example, insulin receptor substrate,[37] mitochondrial proteins,[38] exosome sizes and miRNA cargo,[21]

[1] These authors contributed equally to this work.

and inflammatory markers.[39] This strategy for the diagnosis or evaluation of the therapeutic response may also reveal the molecular mechanism of MDD, consequently identifying potential drug targets.

In our previous study, the "extreme trait strategy" combined with tools of proteomics and bioinformatics was used for the discovery of new biomarkers using plasma and brain tissue of MDD patients. The results revealed a higher plasma level of vitamin D-binding protein (VDBP) in homogeneous MDD patients compared to those in the plasma of well-matched healthy controls (HCs), and its plasma level was significantly correlated to the severity of depressive symptoms, consistent with the measurement in the postmortem brain tissues of the dorsolateral prefrontal cortex (DLPFC) in MDD patients[4]. Therefore, this work aims to evaluate whether the level of VDBP is altered in brain-cell-derived EVs (BCDEVs) of MDD patients compared to HCs, and, if so, whether it can be considered a potential biomarker for the diagnosis of MDD. To reach this goal, the total EVs (TEVs) in the plasma were isolated and identified from the discovery and validation cohorts of first-episode drug-naïve or drug-free MDD patients and HCs. These TEVs were further subjected to immunoprecipitation to capture, detect, characterize, and quantify extracellular vesicles, allowing the differentiation among NDEVs, microglia-derived EVs (MDEVs), and ADEVs. The primary results revealed that the VDBP level was selectively reduced in MDEVs enriched from the plasma of MDD patients compared to that of HCs. Further study on the correlation between the VDBP level of plasma MDEVs and prelimbic (PrL) brain tissues of depressed mice or CSF of depressed rhesus macaques confirmed these results.

Materials and methods

Human subjects and plasma collection

The discovery cohort included 20 HCs and 20 MDD patients who were first-episode drug-naïve or drug-free and diagnosed using the Diagnostic and Statistical Manual of Mental Disorders, Fourth Edition (DSM-IV) and recruited from the Affiliated Zhongda Hospital of Southeast University using a one-to-one matching for high homogeneity. The diagnosis of all patients was reconfirmed as MDD by re-interview in the outpatient department prior to data analysis. The validation cohort consisted of 38 HCs and 88 MDD patients recruited from identical units using the same method. The clinical and neuropsychological assessment of all participants was performed according to the methodology published in our previous article.[4] The demographic and clinical characteristics of participants of the discovery and validation cohorts are summarized in Table S1. Approximately 3 mL of whole blood was collected from each participant between 8:00 a.m. to 9:00 a.m. after overnight fasting and placed into EDTA-coated tubes. The samples were centrifuged at 2000 g for 10 min at 4 °C, and the collected plasma was stored at −80 °C until further use. All participants or their legal guardians provided informed consent. This study was approved by the Ethics Committee of the Affiliated Zhongda Hospital of Southeast University.

Establishment and evaluation of depression-like behavior model and collection of plasma and CSF in rhesus macaques

Rhesus macaque subjects

Six male rhesus macaques (aged 5—8 years, body weight 6—9 kg) were used in the current study. The animals were singly housed in a controlled environment, with a 12 h light/12 h dark cycle. The animals were accommodated in their cages for at least 3 months prior to initial manipulation, and all efforts were made to minimize the monkeys' suffering. All animal procedures were approved by the Institutional Animal Care and Use Committee and performed at the Shenzhen Institute of Advanced Technology, Chinese Academy of Sciences (supplementary materials and methods).

Experimental design

Depression-like behavior was induced in rhesus macaques by exposure to chronic glucocorticoid.[40] Animals were randomly assigned to the glucocorticoid or control group (3 animals in each group), which was subjected to either prednisolone acetate or saline treatment. Prednisolone acetate (15 mg/kg; Zhejiang Xianju Pharmaceutical Co., Ltd, China) was injected intramuscularly daily for 6 weeks. Saline was used to dilute prednisolone acetate injection. The control group received an equivalent volume of saline daily. All injections were performed at 10:00 a.m. The whole behavior and vital signs were monitored and scored by activity monitors throughout the experiment (ActiGraph, LLC., FL, USA), and the body weight, as well as depression-like behaviors and anhedonia, were assessed before (baseline) and after the treatment (test).

Body weight

The body weight of all animals was recorded every two weeks in a monkey chair or during physical examinations.

Quantification of depressive behaviors

The behaviors of the monkeys were recorded by video recorders in the housing room in the morning for three consecutive hours. The time spent in the front of the cage and the back of the cage were recorded and the movement and huddle behaviors were scored. Huddling up was considered a representative phenotype of depression in monkeys because it most effectively reflects the core posture of depression.[41] Depression-like huddling behavior was defined as a fetal-like, self-enclosed posture with the head at or below the shoulders during the waking state.[42,43]

Sucrose preference test

All animals were adapted to a 22 h/day water restriction schedule before the test. Two identical bottles (500 mL) for 2 h per day were provided during the test period; one contained 1.5% sucrose solution (SIGMA, Aldrich, China), and the other contained tap water. The bottle was refilled

and the positions were alternated every 30 min. All tests were performed between 10:00 a.m. and 12:00 p.m. (supplementary materials and methods).

Blood and CSF samples collection

The whole blood and CSF were obtained under Zoletil 50 anesthesia (0.1 mL/kg, intramuscular injection; Virbac S.A., China). All samples were collected at the same time of the day (9:00 a.m. and 10:00 a.m.). The sample preparation procedures are described in previous studies.[40,44] The CSF was obtained through a needle inserted between the 3rd and 4th lumbar vertebrae. Collected blood and CSF samples were stored at −80 °C until further use.

Establishment and evaluation of the depression-like behavior model and collection of plasma and brain tissue in mice

Male adult C57BL/6 mice (23.0—26.0 g, 6—8 weeks old) were purchased from Sino-British SIPPR/BK Lab Animal Ltd. (Shanghai, China) and randomly assigned to two groups. Mice were housed in four per cage at ambient temperature (23 ± 1 °C) and relative humidity (55% ± 2%) and under a 12 h/12 h day/night cycle with free access to food and water. Mice were subjected to a one-week acclimation period prior to experiments. All animal care and experimental procedures were performed in strict accordance with the appropriate institutional ethical guidelines and approved by the Institutional Animal Care and Use Committee of Southeast University. An LPS-induced depression-like behavior mouse model was established according to a previous method.[45] Mice were treated with LPS (1.0 mg/kg, intraperitoneal injection) (LPS group, $n = 12$) or saline (control group, $n = 7$) for 5 successive days.

Sucrose preference test (SPT)

The SPT was used to assess anhedonia, which is a core symptom of depression in mice. The weight of the consumed liquid was measured at the end of the SPT. The sucrose preference value was calculated as the ratio of sucrose solution intake to the total intake of sucrose solution and water (supplementary materials and methods).

Tail suspension test (TST)

The TST is a widely used behavioral despair test. Each mouse was individually suspended 50 cm above the floor using an adhesive tape placed approximately 2 cm from its tail tip for 6 min. The immobility time during the last 4 min was assessed. A longer immobility time indicated a more severe depression-like state.

Forced swim test (FST)

The FST is another widely used behavioral despair test. Briefly, mice were individually forced to swim in a transparent glass cylinder for 6 min. The immobility time during the last 4 min was measured. A longer immobility time indicated a more severe depression-like state (supplementary materials and methods). The TST and FST data were calculated and analyzed using the ANY-Maze behavioral monitoring system (Stoelting Co., Wood Dale, IL, USA).

Collection of mouse plasma and brain tissues

The mice were sedated with 1% pentobarbital at the end of the behavioral test and blood was collected by intracardiac puncture with a syringe containing 15% EDTA. The blood was centrifuged at 1500 g for 15 min at 4 °C, and the obtained plasma was stored at −80 °C until further use. Subsequently, the mice were immediately perfused with cold PBS after blood collection, and then with 4% paraformaldehyde. The whole brain was harvested and fixed overnight in 4% paraformaldehyde. After 48 h of sucrose gradient dehydration, the brain was snap-frozen in optimal cutting temperature compound and stored at −80 °C for further experiment until it was cut into 20 μm-thick slices using a cryostat (CM1900, Leica, Nussloch, Germany).

Isolation and collection of plasma TEVs

TEVs were isolated from the plasma by the ExoQuick precipitation method (System Biosciences Inc., Mountain View, CA) as described in a previous study with slight modifications.[19] Briefly, 0.3 mL plasma was incubated with 0.15 mL thromboplastin-D (ThermoFisher Scientific, Waltham, USA) for 1 h at room temperature, followed by the addition of 0.2 mL calcium- and magnesium-free Dulbecco's balanced salt solution containing a protease inhibitor cocktail (Roche, Indianapolis, IN) and phosphatase inhibitor cocktail (Thermo Fisher Scientific). Then, samples were centrifuged at 10,000 rpm for 5 min at 4 °C and the supernatant was transferred into a clean tube. TEVs were collected from the supernatants by precipitation with ExoQuick and centrifugation at 1500*g* for 30 min at 4 °C. TEVs were resuspended in 200 μL PBS with protease and phosphatase inhibitors. A TEV fraction was kept for characterization.

Immunoprecipitation of EVs using microglial, neuronal, and astrocytic markers

BCDEVs were prepared as previously described with minor modifications.[19] Sixty microliter streptavidin magnetic beads (ThermoFisher Scientific, Waltham, MA, USA) were washed twice with 1 mL of Wash Buffer (TBS containing 0.1% Tween™-20 Detergent). The beads were collected using a magnetic stand (DynaMag-2 Magnet, Product No. 12321D, Thermo Scientific) and re-suspended in 250 μL isolation buffer (0.1% BSA in PBS). The antibody labeling was performed by the incubation of the magnetic beads with 5 μg biotin-labeled antibodies against cell type-specific surface proteins expressed on the exosomes, such as TMEM119 (Cat. No. 853302, BioLegend, San Diego, California, USA) (for MDEV), L1CAM/CD171-Biotin (Cat. No. 13-1919-82, ThermoFisher Scientific) (for NDEV), and GLAST

(Cat. No. ACSA-1-Biotin, Miltenyi Biotec, Auburn, California, USA) (for ADEV), at room temperature for 1 h under continuous mixing. The TEVs were combined with the antibody-labeled magnetic beads and incubated overnight (24 h) at 4 °C under continuous mixing. TMEM119 antibody was labeled with biotin using FluoReporter Mini-biotin-XX protein labeling kit (Invitrogen, Carlsbad, California, USA) following the manufacturer's instructions. Beads were then magnetized and washed four times with 1 mL wash buffer before the final re-suspension in 200 μL PBS containing 1% BSA and protease and phosphatase inhibitors. Finally, 100 μL beads (with attached EVs) were transferred into a separate tube, mixed with 100 μL Elution Buffer (0.1 M glycine, pH 3.0), and incubated at room temperature under 5 min mixing. The beads were magnetically separated and the resulting solutions contained the specific subgroup of exosomes. The pH of the solutions was then adjusted to 7.0 using 1 M Tris—HCl (pH 8.6). The resulting solutions containing the target exosomes were characterized by transmission electron microscopy (TEM) and nanoparticle tracking analysis (NTA). Western blot was used to confirm the presence of exosome-specific molecular markers.

Transmission electron microscopy (TEM) analysis

Twenty μL of BCDEV suspension was loaded onto the fixed carbon grid at room temperature for 3—5 min, and the excess suspension was removed using filter paper. A total of 2% phosphotungstic acid was dropped on the copper grid to stain for 1—2 min and the excess liquid was removed using filter paper before drying at room temperature. The copper grids were washed twice with deionized water and imaged using an HT7800 TEM operated at an acceleration voltage of 80 kV at a magnification of 40,000.

Nanoparticle tracking analysis (NTA)

The particle size of the extracted EVs was evaluated by the nanoparticle tracking analysis device (ZetaView PMX 110, Software version: 8.04.02. SP2, Particle Metrix, Germany).

Immunofluorescence of mouse brain tissue

The brain slices were washed in PBS three times, permeabilized with 0.3% Triton X-100 for 30 min, and blocked with 3% goat serum at room temperature for 1 h. Then, they were incubated overnight with mouse anti-VDBP (1:50, Cat. No. sc-365441, Santa Cruz Biotechnology, Dallas, Texas) and rabbit anti-ionized calcium binding adaptor molecule 1 (Iba1) (1:1000, Cat. No. 019—19741, Wako, Osaka, Japan) antibodies at 4 °C. The brain slices were washed three times in PBS and incubated for 2 h with Alexa Fluor488 secondary antibody for VDBP and Alexa Fluor 594 secondary antibody for Iba1. The brain slides were washed other three times in PBS and stained with DAPI for 10 min. Co-localization fluorescence images were obtained and analyzed using an Olympus microscope (VS200, Olympus, Tokyo, Japan).

Western blot

Plasma EVs were homogenized by RIPA lysis buffer containing protease inhibitor (Beyotime, Shanghai, China) on ice, followed by centrifugation at 12,000 g for 15 min at 4 °C. The protein concentration was measured using the BCA kit (P0010S, Beyotime, Shanghai, China). The proteins in the lysate were separated by SDS-PAGE gels (GenScript, Nanjing, China), and transferred into a PVDF membrane (ISEQ00010, Millipore, Darmstadt, Germany). The membrane was blocked with 5% skimmed milk at room temperature for 1 h, and then incubated with the following primary antibody overnight at 4 °C: Anti-Alix (1:1000, ab275377, Abcam, Cambridge, UK), anti-L1CAM (1:1000, ab208155, Abcam, Cambridge, UK), anti-TMEM119 (1:1000, A20287, ABclonal, Wuhan, China), anti-GLAST (1:1000, ab181036, Abcam, Cambridge, UK), anti-VDBP (16922-1-AP, Proteintech, Rosemont, IL). Next, the membrane was incubated with goat anti-rabbit secondary antibody or goat anti-mouse secondary antibody (Abcam, Cambridge, UK), depending on the source of the primary antibody, at room temperature for 1 h. The blots were visualized using the chemiluminescent reagent (E412, Vazyme, Nanjing, China) under a chemiluminescence image analysis system (Tanon4600, China).

Measurement of VDBP by enzyme-linked immunosorbent assay (ELISA)

After the isolation using magnetic beads, BCDEVs were lysed by adding RIPA buffer directly to the beads. Magnetic beads were then magnetized and removed, and the lysate of the EVs was collected. The VDBP level in the exosome preparation from each brain cell type was normalized to the total protein (measured by the BCA assay) as previously reported.[28] VDBP was measured using a commercial ELISA kit (human and rhesus macaque samples: EH2937, Fine Biotech, China; mouse samples: EK2063, BOSTER, China) in accordance with the manufacturer's protocol. The VDBP level in each plate was calculated according to the standard curve and dilution factor.

Statistical analysis

Statistical analysis was performed using SPSS 23.0 software (SPSS, Inc., Chicago, IL, USA). Categorical variables were analyzed using a chi-squared test, and continuous variables using an independent-sample *t*-test when normally distributed, otherwise using a Mann—Whitney *U* test. The receiver operator characteristic (ROC) curve and area under the curve (AUC) were used to determine the diagnostic accuracy of the protein biomarkers. The correlation between the HAMD24 score and BCDEV-VDBP level was evaluated using Pearson's correlation analysis. Results are expressed as mean ± standard error of the mean (SEM). SQRT transformation of the VDBP values was performed when required to improve the normalization of the data for statistical analysis, and the corresponding values were presented as SQRT values. A *P*-value of less than 0.05 ($P < 0.05$, two-tailed) was considered statistically significant.

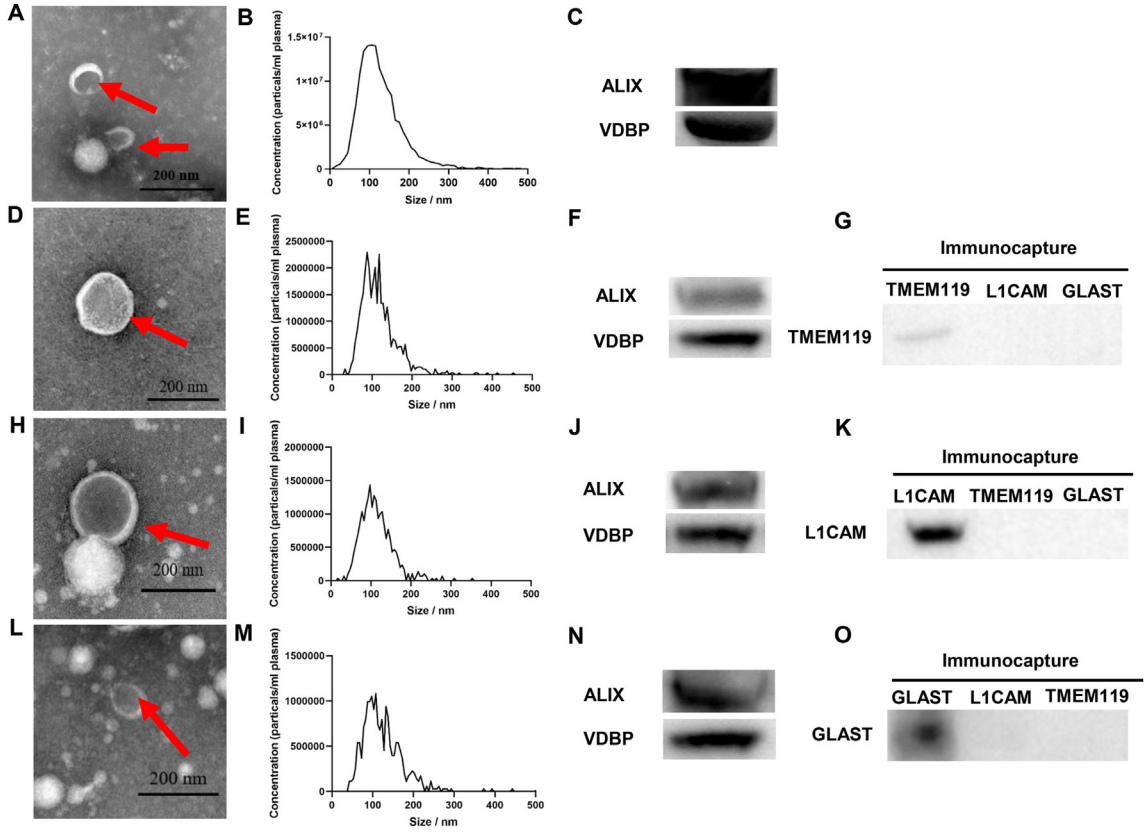

Figure 1 Characterization of total TEVs and BCDEVs isolated from human plasma. **(A)** Representative TEM images of TEVs isolated from human plasma. Exosomes are indicated by red arrows. Scale bar = 200 nm. **(B)** NTA of TEs. **(C)** Western blot of the common exosome marker ALIX and VDBP in TEVs. **(D)** Representative TEM of MDEVs. The exosome is indicated by red arrows. Scale bar = 200 nm. **(E)** NTA showing the size and distribution of MDEVs. **(F)** Western blot of the common exosome marker ALIX and VDBP in MDEVs. **(G)** Western blot showed that the microglia marker TMEM119 was selectively expressed in MDEVs. **(H)** Representative TEM of NDEVs. The exosome is indicated by a red arrow. Scale bar = 200 nm. **(I)** NTA showing the size and distribution of NDEVs. **(J)** Western blot identifying the common exosome marker ALIX and VDBP in NDEVs. **(K)** Western blot showing the neuron marker L1CAM selectively expressed in NDEVs. **(L)** Representative TEM of ADEVs. Exosomes are indicated by red arrows. Scale bar = 200 nm. **(M)** NTA showing the sizes and distribution of ADEVs. **(N)** Western blot identifying the common exosome marker ALIX and VDBP in ADEVs. **(O)** Western blot showing the astrocyte marker GLAST selectively expressed in ADEVs.

Results

Isolation and characterization of plasma TEVs and BCDEVs

The method described in a previous study was used to enrich BCDEVs from peripheral blood.[19] Plasma TEVs (Fig. 1A—C) were isolated, and then TMEM119-positive MDEVs (Fig. 1D—G), L1CAM-positive NDEVs (Fig. 1H—K), and GLAST-positive ADEVs (Fig. 1L—O) from plasma TEVs were subsequently isolated by immunoprecipitation method. The characterization of TEVs and BCDEVs was performed by TEM, NTA, and Western blot. TEM showed the morphology of EVs (Fig. 1A, D, H, L). NTA revealed that the EV size was approximately 100 nm (Fig. 1B, E, I, M). ALIX, a commonly used marker for exosome identification, was enriched in both plasma TEVs (Fig. 1C) and BCDEVs (Fig. 1F, J, N). Western blot using specific markers of BCDEVs showed that TMEM119, L1CAM, and GLAST were specifically expressed in MDEVs (Fig. 1G), NDEVs (Fig. 1K), and ADEVs (Fig. 1O) respectively.

Clinical features of the discovery and validation cohorts

In the clinical study, the VDBP level was detected in three types of BCDEVs enriched from plasma in the discovery and validation cohorts of MDD patients and HCs, whose characteristics are listed in Table S1. In the discovery and validation cohorts, no significant difference was found between subjects with MDD and HCs in age, gender, BMI, and education years except for the Hamilton Depression Rating Scale-24 item (HAMD-24) scores.

Altered VDBP level in plasma MDEVs between MDD patients and HCs in the discovery and validation cohorts

No significant difference in VDBP concentration was found between that in plasma TEVs from MDD patients and HCs in both the discovery (Fig. S1A) and validation cohorts (Fig. S1B). This result demonstrated a poor diagnostic performance (Fig. S1C) with no significant association with

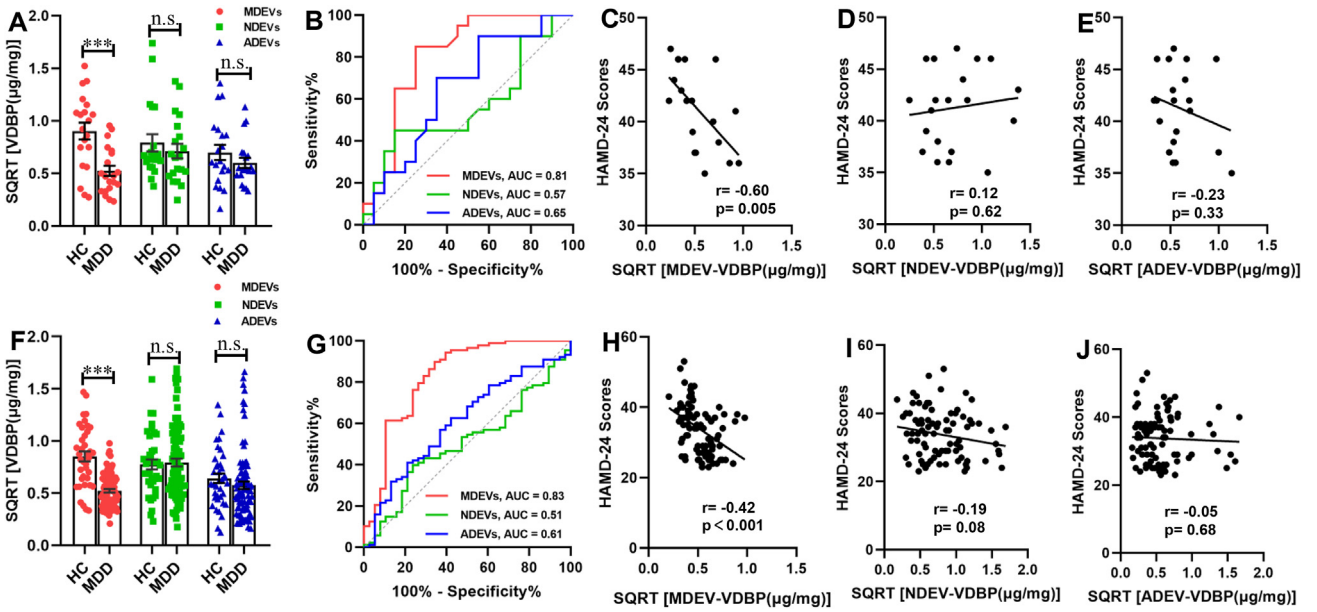

Figure 2 Concentration and diagnostic performance of VDBP in plasma BCDEVs from MDD patients and HCs. **(A)** VDBP protein level in plasma MDEVs, NDEVs, and ADEVs from MDD and HCs in the discovery cohort, as measured by ELISA. **(B)** Diagnostic accuracy of VDBP in plasma BCDEVs of MDD in the discovery cohort, as calculated by the AUC of the ROC curve. Pearson correlation analysis showed the relationships between the VDBP level in plasma MDEVs **(C)**, NDEVs **(D)**, or ADEVs **(E)** and HAMD-24 scores in MDD patients of the discovery cohort. **(F)** VDBP level in plasma MDEVs from MDD patients was confirmed in the validation cohort. **(G)** Diagnostic accuracy of VDBP in plasma BCDEVs of MDD in the validation cohort. Pearson correlation analysis showed the relationships between VDBP level in plasma MDEVs **(H)**, NDEVs **(I)**, or ADEVs **(J)** and HAMD-24 scores in MDD patients of the validation cohort. HAMD-24: Hamilton Depression Rating Scale-24 item. ***$P < 0.001$, n. s.: = not significant. Results are presented as mean ± SEM.

HAMD-24 score (Fig. S1D, E) in both cohorts. After immunocapture by cell-specific markers from TEVs, the VDBP level in plasma MDEVs (MDEV-VDBP) from MDD patients in the discovery cohort significantly decreased compared to that in the plasma MDEVs of well-matched HCs (Fig. 2A), which was further confirmed in an independent large validation cohort with first-episode drug-naïve or drug-free patients and HCs (Fig. 2F). Pearson correlation analysis showed that the MDEV-VDBP level was significantly and negatively correlated with the HAMD-24 score in the patients of both cohorts (Fig. 2C, $r = -0.60$, $P = 0.005$; Fig. 2H, $r = -0.42$, $P < 0.001$). Importantly, the MDEV-VDBP level discriminated MDD from HCs with an AUC of 0.81 (sensitivity = 85.00%, specificity = 75.00%) and 0.83 (sensitivity = 89.80%, specificity = 65.80%) in the discovery (Fig. 2B) and validation cohorts (Fig. 2H) respectively.

Unchanged VDBP level in plasma ADEVs and NDEVs of MDD from both discovery and validation cohorts

No statistical difference in VDBP level in MDD plasma ADEVs (ADEV-VDBP) from both the discovery and validation cohorts compared with the HCs, and no correlation between the ADEV-VDBP level and HAMD-24 score in both cohorts ($r = -0.23$, $P = 0.33$; $r = -0.05$, $P = 0.68$, respectively; Fig. 2E, J) were found. The AUCs of the ADEV-VDBP were 0.65 (sensitivity = 70.00%, specificity = 65.00%) in the discovery cohort (Fig. 2B) and 0.61 (sensitivity = 62.50%, specificity = 57.90%) in the validation cohort (Fig. 2G).

Like the observed results of ADEVs, no statistical difference in the plasma VDBP level of NDEVs (NDEV-VDBP) between MDD and HCs and no significant correlation between the NDEV-VDBP level and HAMD-24 score in the discovery (Fig. 2D, $r = 0.12$, $P = 0.62$) and validation cohorts (Fig. 2I) ($r = -0.19$, $P = 0.08$) were found. The AUCs of the NDEV-VDBP were 0.57 (sensitivity = 45.00%, specificity = 85.00%) and 0.51 (sensitivity = 39.80%, specificity = 76.30%) in the discovery (Fig. 2B) and validation cohorts (Fig. 2G), which were far from the standard value as a potential diagnostic biomarker.

Taken together, the above experiments on plasma BCDEVs suggested that VDBP only in plasma MDEVs might serve as a potential diagnostic biomarker for MDD with higher diagnostic accuracy. Since no significant correlation of VDBP with MDD was observed in NDEVs or ADEVs, our attention focused on VDBP in MDEVs in subsequent animal experiments.

Altered VDBP level in plasma MDEVs and CSF of depressed rhesus macaques

Since the biopsy or autopsy of brain tissue and CSF from MDD patients is difficult to be obtained, a depression-like rhesus macaque model was used to further verify whether plasma MDEV-VDBP was consistent with CSF-VDBP level. Depressive behaviors, including decreased sucrose preference (Fig. 3A) and accumulated behaviors (Fig. 3B), were observed in chronic glucocorticoid-treated rhesus macaques. Plasma MDEVs from rhesus macaques were isolated by immunoprecipitation and characterized by NTA, TEM, and Western blot (Fig. 3C–E). The plasma MDEV-VDBP (Fig. 3F) and CSF-VDBP (Fig. 3G) levels were not significantly different between control and chronic

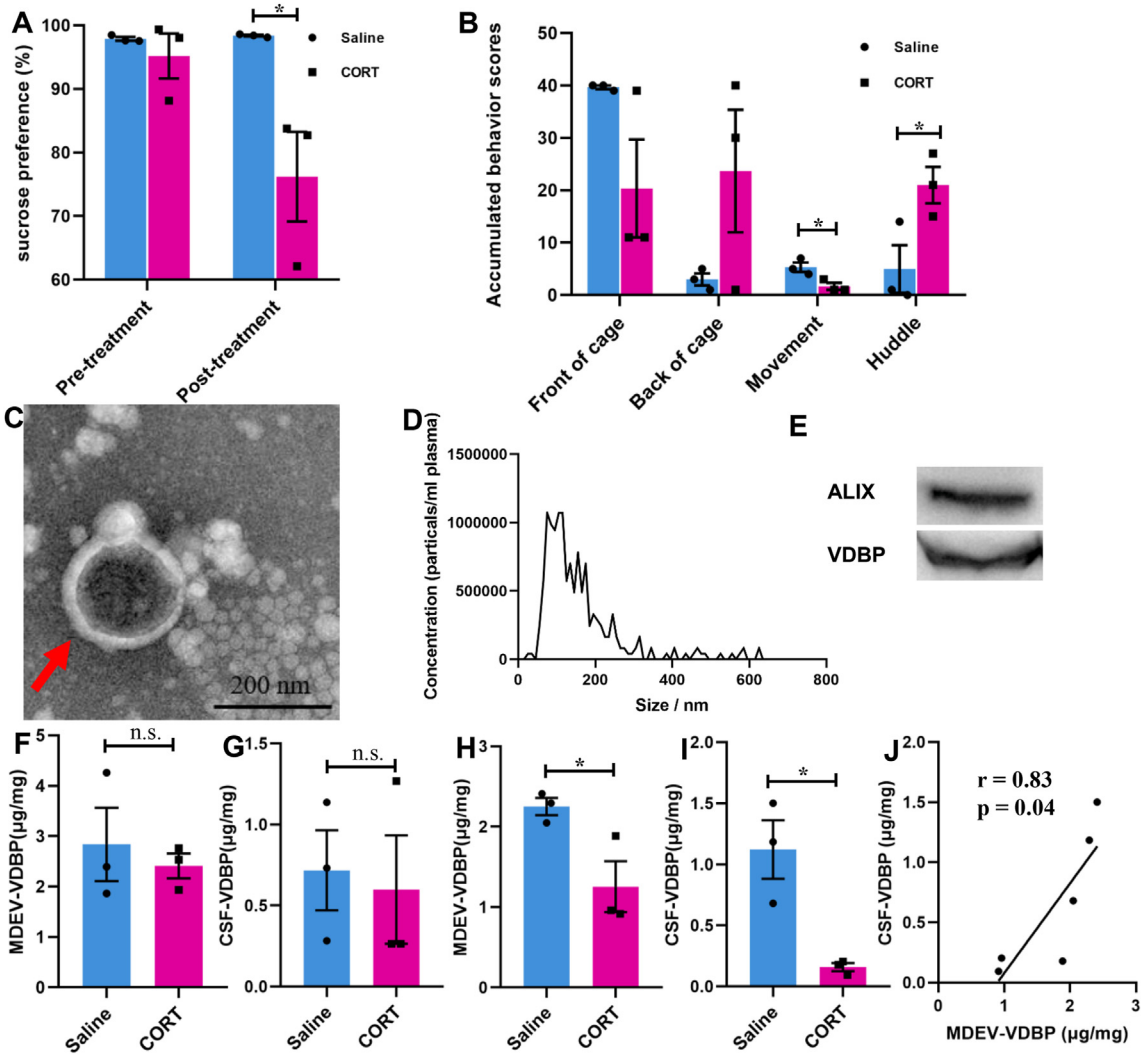

Figure 3 Characterization and VDBP evaluation of plasma MDEVs from chronic glucocorticoid-induced depressed rhesus macaque model. **(A)** Sucrose preference test (SPT) and **(B)** accumulated behavior scores of chronic glucocorticoid and saline-treated rhesus macaque. Isolated plasma MDEVs from rhesus macaque were characterized by TEM **(C)** and NTA **(D)**. The red arrow indicates MDEVs in a representative TEM image. **(E)** Western blot showing the presence of the exosome marker ALIX and VDBP in isolated rhesus macaque plasma MDEVs. VDBP concentrations in plasma MDEVs **(F)** and cerebrospinal fluid (CSF) **(G)** of rhesus macaque at baseline were measured by ELISA. VDBP concentrations in plasma MDEVs **(H)** and CSF **(I)** of rhesus macaque after saline or chronic glucocorticoid treatment were measured by ELISA. **(J)** Pearson correlation analysis showing the relationships between VDBP in plasma MDEVs and CSF of rhesus macaque after treatment with saline or chronic glucocorticoid. $^*P < 0.05$, n. s. = not significant. Results are presented as mean ± SEM.

glucocorticoid-treated groups at baseline. The VDBP levels in plasma MDEVs (Fig. 3H) and CSF (Fig. 3I) after chronic glucocorticoid induction were markedly decreased compared with those in the control group. Pearson correlation analysis showed a positive correlation between the VDBP level in plasma MDEVs and that in CSF from saline or chronic glucocorticoid-treated rhesus macaques (Fig. 3J).

Altered VDBP level in plasma MDEVs and microglia in PrL brain region of LPS-induced depression-like behavior mice

Our previous study found that VDBP is significantly increased in DLPFC of MDD patients,[4] and the prelimbic cortex of rodents is a functional analog of DLPFC in humans.[46] Therefore, the alteration of VDBP was evaluated in microglia of PrL and plasma MDEVs of LPS-induced depression-like mice. The workflow of the LPS-induced depression-like mice model and the behavioral evaluation methods are schematized in Figure 4A. Intraperitoneal injection of LPS for 5 continuous days led to reduced body weight (Fig. 4B) and sucrose preference (Fig. 4C) together with increased immobile time in TST (Fig. 4D) and FST (Fig. 4E). Mouse plasma MDEVs were isolated using the method described in the materials and methods, sections of immunoprecipitation (IP) of EVs using microglial markers (Fig. 4F—H) and the levels of VDBP in MDEVs were quantified by ELISA. The results showed that the level of plasma MDEV-VDBP in LPS-induced depression-like mice was significantly lower than that in the control group (Fig. 4I).

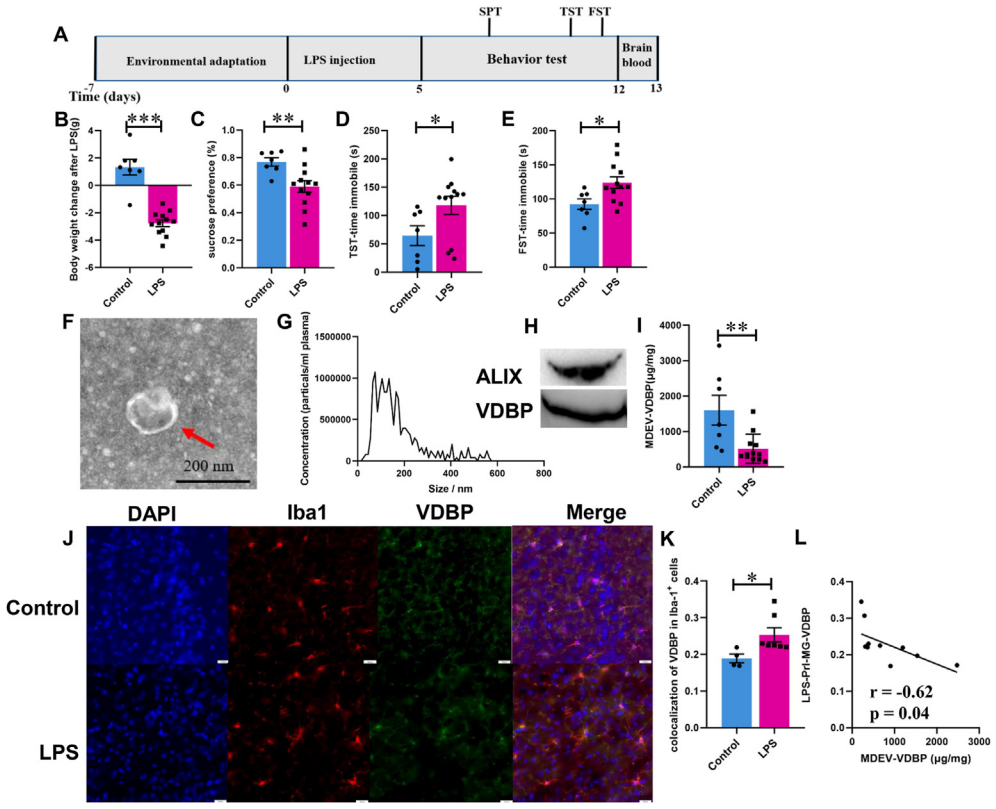

Figure 4 VDBP level in plasma MDEVs and microglia in PrL of LPS-induced depressed mice. **(A)** Schematic diagram of the experimental procedure for LPS-induced depressed mouse model. **(B)** Body weight loss in LPS-induced depressed mice. Sucrose preference test **(C)**, tail suspension test **(D)**, and forced swimming test **(E)** of mice treated with saline (Control) or LPS. Isolation and characterization of plasma MDEVs by TEM **(F)**, NTA **(G)** of LPS-induced depressed mice. The red arrow points to the plasma MDEV successfully isolated. **(H)** Western blotting showing the enriched VDBP and exosome marker ALIX in isolated mice plasma MDEVs. **(I)** VDBP in plasma MDEVs from LPS-induced depressed mice as measured by ELISA. **(J)** Immunofluorescence images showing the microglial VDBP level (green) in the PrL of LPS-induced depressed mice. The nucleus was stained with DAPI (blue). Microglia were labeled with Iba-1 antibody (red). **(K)** Colocalization of VDBP in Iba-1^{+} cells was calculated. **(L)** Pearson correlation analysis showing the relationships between VBBP in plasma MDEVs and PrL microglia. $^{*}P < 0.05$, $^{**}P < 0.01$, $^{***}P < 0.001$. Results are presented as mean ± SEM.

Subsequently, increased microglial VDBP expression was found in the PrL region from LPS-induced depression-like mice compared with the saline-treated control group (Fig. 4J, K), consistent with our previous finding that VDBP is selectively up-regulated in DLPFC of MDD patients.[4] The level of VDBP in plasma MDEVs was negatively correlated to that in PrL microglia (Fig. 4L).

Discussion

This study is the first study to report that VDBP in plasma MDEVs of MDD patients was selectively and significantly reduced and observably associated with the severity of depressive symptoms. Moreover, the decreased plasma MDEV-VDBP in chronic glucocorticoid-treated rhesus macaques and depression-like behavior mice was significantly correlated with the VDBP level in the CSF of the macaque model or the microglia VDBP level in the PrL brain region of the mouse model, respectively, suggesting that plasma MDEV-VDBP might be a potential diagnostic biomarker of MDD that might represent the CNS.

Regarding the advantage of the methodology and technology in the present study, first, the "discovery" and "validation" cohorts of this study strictly enrolled patients who were first-episode drug-naïve or drug-free with more than 2-week washout period for antidepressants, as well as strictly matched HCs, reducing the effects of drugs and long-term disease duration and improving subject homogeneity. Second, plasma TEVs and three important BCDEVs were successfully isolated and identified using a series of internationally recognized technical means and methods. In particular, MDEVs were isolated and identified and MDEV-VDBP levels were measured for the first time in human plasma, and VDBP levels were compared and analyzed in three BCDEVs. The results revealed that plasma MDEV-VDBP was significantly and selectively reduced in MDD patients, which was further verified in chronic glucocorticoid-treated rhesus macaques and depression-like mice. Moreover, the correlations between the decreased VDBP levels in plasma MDEVs and the increased microglial VDBP in the PrL region of the mouse model or the decreased VDBP in the CSF of the rhesus macaque model were analyzed. In sum, the

scientific, rigorous, and feasible methodology improved the credibility of the findings.

As mentioned above, our previous studies consistently found that VDBP levels in plasma and postmortem brain tissue in the DLPFC region were selectively significantly increased in MDD patients,[4] suggesting that VDBP is a potential candidate molecule for the diagnosis of MDD. The present study focused on plasma BCDEVs and found that MDEV-VDBP was selectively reduced in MDD patients. Further studies from depression-like mice or rhesus macaques confirmed that decreased plasma MDEV-VDBP was significantly associated with increased microglia VDBP in the PrL region or decreased VDBP in the CSF, respectively, suggesting a correlative discovery between the CNS and the peripheral blood in animal models of depression. The above evidence suggested that plasma MDEV-VDBP might be a more accurate candidate biomarker in the diagnosis of MDD.

As we know, the first studies published in 2014,[22] 2016,[17] and 2020[23] successfully isolated and identified candidate molecules in NDEVs, ADEVs, and oligodendrocyte-derived extracellular vesicles (ODEVs) from peripheral blood, respectively, such as α-synuclein, Aβ42, and confirmed that they can represent the CNS. Gradually increasing evidence revealed that the candidate molecules in peripheral blood BCDEVs are biomarkers for the diagnosis and differential diagnosis of CNS diseases including AD,[17,20,24–27] PD[18,22,28–32], and MSA.[23,28] Four independent recent studies reported abnormal levels of insulin receptor substrate 1(IRS-1),[37] mitochondrial proteins[38] in plasma NDEVs, and of inflammatory markers[39] in serum ADEVs of MDD patients compared to HCs, while changes in plasma NDEV-size and miRNA cargo are associated with the antidepressive response in MDD patients.[21] Until 2021, some scholars first established a method to determine a series of candidate molecules in peripheral blood MDEVs in the cynomolgus monkey model of long-term oxycodone self-administration and detected VDBP.[19] However, up to now, no officially published research is available on the establishment of the human peripheral blood MDEV method and the role of MDEV candidate molecules in disease diagnosis. In this study, MDEV-VDBP was successfully measured in human plasma for the first time based on the above cynomolgus monkey methodology, and the levels of plasma MDEV-VDBP in mice and rhesus macaques were verified across species. Type-I transmembrane protein 119 (TMEM119) is selectively expressed in microglia but not in other brain cells or macrophages, and it is enriched in plasma MDEVs, thus, it was used as a cell type-specific marker of MDEVs in this study.[47–50] However, this study did not simultaneously measure VDBP in brain tissue even CSF in MDD patients to directly analyze central and peripheral correlations. In addition, VDBP levels in CSF of depressed rhesus macaques should include VDBP in various nerve cell subtypes, not just microglia, although previous studies have also analyzed the correlation between candidate molecules in the CSF and peripheral blood NDEVs to determine their central and peripheral correlations (*e.g.*, AD,[20] PD[22]). However, further determination of candidate molecules in different BCDEVs in CSF should be more accurate and worth trying. Therefore, the current findings of this study still need to be viewed with caution.

It is well known that approximately 95% of peripheral circulating VDBP is produced by liver parenchymal cells. Except for its functions related to vitamin D transport, vitamin D-independent functions include the sequestration of actin, modulation of immune and inflammatory responses, binding of fatty acids, and binding to megalin-cubilin receptor complex.[51,52] Unfortunately, little is known about CNS synthesis and metabolism, the distribution of brain regions and nerve cell subtypes, as well as the physiological function and pathological mechanism of VDBP. Indeed, since the late 1980s, VDBP has been reported as expressed in fetal, adult, rat, and mouse brain tissue.[53–57] Some scholars speculated that the paraventricular nucleus (PVN), supraoptic nucleus (SON), and periventricular nucleus (PEV) of the hypothalamus of rats may be the VDBP-producing region.[58] Up to now, only one research group reported that VDBP is colocalized with Aβ plaques, and increasing VDBP significantly attenuates the Aβ accumulation in AD mouse model.[59,60] Serial studies reported abnormalities of VDBP levels in the CSF, including AD,[61] PD,[62] epilepsy,[63] encephalitis,[64] and MS.[65,66] As regards MDD, two plasma proteomic analyses found that VDBP is highly expressed in MDD patients,[67,68] and little else is known. Our previous study found that VDBP levels in plasma and DLPFC brain region of autopsy brain tissue in MDD patients were significantly increased, based on hypothetic-free proteomics and multiple validations.[4] Subsequently, in addition to further identification of the potential role of VDBP as a diagnostic biomarker for MDD in this study, our attention over the past three years focused on elucidating layer by layer the causal mechanisms of the cellular and molecular mechanism of specific brain regions and neural circuits responsible for microglia-VDBP-induced neuronal damage and depression using *ex vivo* cells and animal models combined with microglia-conditional VDBP gene knockout or microglia -overexpressing VDBP mice.

This study is a preliminary and innovative exploratory study. Limitations and future research directions mainly include the following aspects. Firstly, the main findings of this study need to be validated in multiple clinical centers, and a longitudinal follow-up is needed to determine whether VDBP abnormality is a "state" or a "feature". In addition, repeated validation is needed in different subgroups throughout the life cycle to determine its specificity or selectivity. Secondly, mouse model and rhesus macaques have been used to explore the correlation between central and peripheral VDBP due to the difficulty of obtaining brain tissue even CSF from MDD patients, but despite that, follow-up studies still need to be performed to confirm the results in CSF or brain tissue samples from MDD patients. VDBP molecular probes should be developed to detect the specific accumulation or expression changes of VDBP brain regions and nerve cell subtypes *in vivo* using positron emission tomography. Thirdly, it is urgent to clarify the potential mechanism of the increase of VDBP in brain microglia and the decrease of VDBP in peripheral microglia-derived EVs. As mentioned above, is there an increase in VDBP accumulation in brain microglia? Or the transport through the BBB to the periphery is blocked? Or is it transported to the periphery by other routes such as the lymphoid system? In addition, it is also necessary to compare and analyze the sensitivity,

specificity, and accuracy of VDBP as a biomarker for the diagnosis of MDD in biological samples from different sources, including peripheral blood, peripheral blood TEVs, or BCDEVs, so as to promote the development and translation of diagnostic kits. Fourthly, the CNS anabolism and physiological function of VDBP, especially its mechanism in the occurrence of MDD, as well as the two-way regulation of central and peripheral hepatogenic VDBP should be urgently clarified. Only by obtaining sufficient evidence of multi-level upstream research, it is possible to determine the potential role of VDBP diagnostic biomarkers and identify new targets for drug and neuroregulatory interventions.

In conclusion, the main findings of this study suggest that the plasma MDEV-VDBP may be a potential candidate biomarker in the diagnosis of MDD. However, these temporary findings should be considered with caution.

Copyright Transfer Agreement

The authors of the article (Title: Vitamin D-binding protein in plasma microglia-derived extracellular vesicles as a potential biomarker for major depressive disorder) agrees to transfer the copyright to Elsevier.

Author contributors

ZZ and YK conceived the study and guided the experiment. GZ and LL performed the experiments. GZ and LL jointly completed the experimental data collection and statistical analysis. GZ and LL prepared the figures and tables. ZZ, YK, and GZ drafted the manuscript. ZZ and YK revised, reviewed, and edited the draft. DX, JJ, DF, and CX provided technical help. YB, ZL, and ZZ completed the whole rhesus macaque-related study, including the depression modeling, behavioral evaluation, and collection of cerebrospinal fluid and blood with the guidance of ZM, JD, and XL. All authors read and accepted the final version of the manuscript.

Conflict of interests

The authors declare no competing financial interests in relation to the work described.

Funding

This study was supported by the National Natural Science Key Foundation of China (No. 81830040 and 82130042 to ZJ Zhang), China Science and Technology Innovation 2030 - Major Project (China) (No. 2022ZD0211701, 2022ZD0211700 and 2021ZD0200700 to ZJ Zhang), Science and Technology Program of Guangdong, China (No. 2018B030334001 to ZJ Zhang), and Science and Technology Program of Shenzhen, China (No. GJHZ20210705141400002, KCXFZ20211020164543006, JCYJ20220818101615033 and ZDSYS20220606100606014 to ZJ Zhang) and The National Natural Science Foundation of China (No. U20A6005 to ZQM).

Acknowledgements

We would like to thank our colleagues from the Department of Neurology, Affiliated Zhongda Hospital of Southeast University, and the Department of Psychiatry, Second Affiliated Hospital of Xinxiang Medical University for their help during the study. We would also like to thank all study participants, without whom this research would not have been possible. We thank Servicebio Co., Ltd. for its assistance during the study.

Appendix A. Supplementary data

Supplementary data to this article can be found online at https://doi.org/10.1016/j.gendis.2023.02.049.

References

1. Kitanaka J, Ecks S, Wu HYJ. The social in psychiatries: depression in Myanmar, China, and Japan. *Lancet*. 2021; 398(10304):948—949.
2. Santomauro DF, Mantilla Herrera AM, Shadid J, et al. Global prevalence and burden of depressive and anxiety disorders in 204 countries and territories in 2020 due to the COVID-19 pandemic. *Lancet*. 2021;398(10312):1700—1712.
3. Huang C, Huang L, Wang Y, et al. 6-month consequences of COVID-19 in patients discharged from hospital: a cohort study. *Lancet*. 2021;397(10270):220—232.
4. Shi Y, Song R, Wang L, et al. Identifying plasma biomarkers with high specificity for major depressive disorder: a multi-level proteomics study. *J Affect Disord*. 2020;277:620—630.
5. Kennis M, Gerritsen L, van Dalen M, et al. Prospective biomarkers of major depressive disorder: a systematic review and meta-analysis. *Mol Psychiatr*. 2020;25(2):321—338.
6. Gururajan A, Clarke G, Dinan TG, et al. Molecular biomarkers of depression. *Neurosci Biobehav Rev*. 2016;64:101—133.
7. Menezes IC, von Werne Baes C, Lacchini R, et al. Genetic biomarkers for differential diagnosis of major depressive disorder and bipolar disorder: a systematic and critical review. *Behav Brain Res*. 2019;357—358:29—38.
8. Hernandez-Baixauli J, Puigbò P, Abasolo N, et al. Alterations in metabolome and microbiome associated with an early stress stage in male Wistar rats: a multi-omics approach. *Int J Mol Sci*. 2021;22(23):12931.
9. Bu T, Qiao Z, Wang W, et al. Diagnostic biomarker Hsa_circ_0126218 and functioning prediction in peripheral blood monocular cells of female patients with major depressive disorder. *Front Cell Dev Biol*. 2021;9:651803.
10. Martins-de-Souza D. Proteomics, metabolomics, and protein interactomics in the characterization of the molecular features of major depressive disorder. *Dialogues Clin Neurosci*. 2014; 16(1):63—73.
11. McCarron RM, Shapiro B, Rawles J, et al. Depression. *Ann Intern Med*. 2021;174(5):ITC65—ITC80.
12. Enache D, Pariante CM, Mondelli V. Markers of central inflammation in major depressive disorder: a systematic review and meta-analysis of studies examining cerebrospinal fluid, positron emission tomography and post-mortem brain tissue. *Brain Behav Immun*. 2019;81:24—40.
13. Shi M, Sheng L, Stewart T, et al. New windows into the brain: central nervous system-derived extracellular vesicles in blood. *Prog Neurobiol*. 2019;175:96—106.
14. Kalluri R, LeBleu VS. The biology, function, and biomedical applications of exosomes. *Science*. 2020;367(6478):eaau6977.

15. Escudé Martinez de Castilla P, Tong L, Huang C, et al. Extracellular vesicles as a drug delivery system: a systematic review of preclinical studies. *Adv Drug Deliv Rev*. 2021;175:113801.
16. Duarte-Silva E, Oriá AC, Mendonça IP, et al. Tiny in size, big in impact: extracellular vesicles as modulators of mood, anxiety and neurodevelopmental disorders. *Neurosci Biobehav Rev*. 2022;135:104582.
17. Goetzl Edward J, Maja M, Dimitrios K, et al. Cargo proteins of plasma astrocyte-derived exosomes in Alzheimer's disease. *FASEB J*. 2016;30(11):3853—3859.
18. Shi M, Kovac A, Korff A, et al. CNS tau efflux via exosomes is likely increased in Parkinson's disease but not in Alzheimer's disease. *Alzheimers Dement*. 2016;12(11):1125—1131.
19. Kumar A, Kim S, Su Y, et al. Brain cell-derived exosomes in plasma serve as neurodegeneration biomarkers in male cynomolgus monkeys self-administrating oxycodone. *EBioMedicine*. 2021;63:103192.
20. Jia L, Qiu Q, Zhang H, et al. Concordance between the assessment of Aβ42, T-tau, and P-T181-tau in peripheral blood neuronal-derived exosomes and cerebrospinal fluid. *Alzheimers Dement*. 2019;15(8):1071—1080.
21. Saeedi S, Nagy C, Ibrahim P, et al. Neuron-derived extracellular vesicles enriched from plasma show altered size and miRNA cargo as a function of antidepressant drug response. *Mol Psychiatr*. 2021;26(12):7417—7424.
22. Shi M, Liu C, Cook TJ, et al. Plasma exosomal α-synuclein is likely CNS-derived and increased in Parkinson's disease. *Acta Neuropathol*. 2014;128(5):639—650.
23. Yu Z, Shi M, Stewart T, et al. Reduced oligodendrocyte exosome secretion in multiple system atrophy involves SNARE dysfunction. *Brain*. 2020;143(6):1780—1797.
24. Fiandaca MS, Kapogiannis D, Mapstone M, et al. Identification of preclinical Alzheimer's disease by a profile of pathogenic proteins in neurally derived blood exosomes: a case-control study. *Alzheimers Dement*. 2015;11(6):600—607.
25. Goetzl EJ, Schwartz JB, Abner EL, et al. High complement levels in astrocyte-derived exosomes of Alzheimer disease. *Ann Neurol*. 2018;83(3):544—552.
26. Goetzl EJ, Boxer A, Schwartz JB, et al. Altered lysosomal proteins in neural-derived plasma exosomes in preclinical Alzheimer disease. *Neurology*. 2015;85(1):40—47.
27. Agliardi C, Guerini FR, Zanzottera M, et al. SNAP-25 in serum is carried by exosomes of neuronal origin and is a potential biomarker of Alzheimer's disease. *Mol Neurobiol*. 2019;56(8):5792—5798.
28. Dutta S, Hornung S, Kruayatidee A, et al. α-Synuclein in blood exosomes immunoprecipitated using neuronal and oligodendroglial markers distinguishes Parkinson's disease from multiple system atrophy. *Acta Neuropathol*. 2021;142(3):495—511.
29. Athauda D, Gulyani S, Karnati HK, et al. Utility of neuronal-derived exosomes to examine molecular mechanisms that affect motor function in patients with Parkinson disease: a secondary analysis of the exenatide-PD trial. *JAMA Neurol*. 2019;76(4):420—429.
30. Jiang C, Hopfner F, Katsikoudi A, et al. Serum neuronal exosomes predict and differentiate Parkinson's disease from atypical Parkinsonism. *J Neurol Neurosurg Psychiatry*. 2020;91(7):720—729.
31. Niu M, Li Y, Li G, et al. A longitudinal study on α-synuclein in plasma neuronal exosomes as a biomarker for Parkinson's disease development and progression. *Eur J Neurol*. 2020;27(6):967—974.
32. Zhao ZH, Chen ZT, Zhou RL, et al. Increased DJ-1 and α-synuclein in plasma neural-derived exosomes as potential markers for Parkinson's disease. *Front Aging Neurosci*. 2019;10:438.
33. Hamlett ED, Goetzl EJ, Ledreux A, et al. Neuronal exosomes reveal Alzheimer's disease biomarkers in Down syndrome. *Alzheimers Dement*. 2017;13(5):541—549.
34. Goetzl EJ, Elahi FM, Mustapic M, et al. Altered levels of plasma neuron-derived exosomes and their cargo proteins characterize acute and chronic mild traumatic brain injury. *Faseb J*. 2019;33(4):5082—5088.
35. Goetzl EJ, Peltz CB, Mustapic M, et al. Neuron-derived plasma exosome proteins after remote traumatic brain injury. *J Neurotrauma*. 2020;37(2):382—388.
36. Winston CN, Romero HK, Ellisman M, et al. Assessing neuronal and astrocyte derived exosomes from individuals with mild traumatic brain injury for markers of neurodegeneration and cytotoxic activity. *Front Neurosci*. 2019;13:1005.
37. Nasca C, Dobbin J, Bigio B, et al. Insulin receptor substrate in brain-enriched exosomes in subjects with major depression: on the path of creation of biosignatures of central insulin resistance. *Mol Psychiatr*. 2021;26(9):5140—5149.
38. Goetzl EJ, Wolkowitz OM, Srihari VH, et al. Abnormal levels of mitochondrial proteins in plasma neuronal extracellular vesicles in major depressive disorder. *Mol Psychiatr*. 2021;26(12):7355—7362.
39. Xie XH, Lai WT, Xu SX, et al. Hyper-inflammation of astrocytes in patients of major depressive disorder: evidence from serum astrocyte-derived extracellular vesicles. *Brain Behav Immun*. 2023;109:51—62.
40. Qin D, Li Z, Li Z, et al. Chronic glucocorticoid exposure induces depression-like phenotype in rhesus macaque (*Macaca mulatta*). *Front Neurosci*. 2019;13:188.
41. Felger JC, Alagbe O, Hu F, et al. Effects of interferon-alpha on rhesus monkeys: a nonhuman primate model of cytokine-induced depression. *Biol Psychiatr*. 2007;62(11):1324—1333.
42. Harlow HF, Suomi SJ. Social recovery by isolation-reared monkeys. *Proc Natl Acad Sci U S A*. 1971;68(7):1534—1538.
43. Shively CA, Register TC, Friedman DP, et al. Social stress-associated depression in adult female cynomolgus monkeys (*Macaca fascicularis*). *Biol Psychol*. 2005;69(1):67—84.
44. Davenport MD, Tiefenbacher S, Lutz CK, et al. Analysis of endogenous cortisol concentrations in the hair of rhesus macaques. *Gen Comp Endocrinol*. 2006;147(3):255—261.
45. Zhang Y, Du L, Bai Y, et al. CircDYM ameliorates depressive-like behavior by targeting miR-9 to regulate microglial activation via HSP90 ubiquitination. *Mol Psychiatr*. 2020;25(6):1175—1190.
46. Lu QB, Sun JF, Yang QY, et al. Magnetic brain stimulation using iron oxide nanoparticle-mediated selective treatment of the left prelimbic cortex as a novel strategy to rapidly improve depressive-like symptoms in mice. *Zool Res*. 2020;41(4):381—394.
47. Ruan C, Elyaman W. A new understanding of TMEM119 as a marker of microglia. *Front Cell Neurosci*. 2022;16:902372.
48. Bennett ML, Bennett FC, Liddelow SA, et al. New tools for studying microglia in the mouse and human CNS. *Proc Natl Acad Sci U S A*. 2016;113(12):E1738—E1746.
49. Satoh JI, Kino Y, Asahina N, et al. TMEM119 marks a subset of microglia in the human brain. *Neuropathology*. 2016;36(1):39—49.
50. Bohnert S, Seiffert A, Trella S, et al. TMEM119 as a specific marker of microglia reaction in traumatic brain injury in postmortem examination. *Int J Leg Med*. 2020;134(6):2167—2176.
51. Speeckaert MM, Speeckaert R, van Geel N, et al. Vitamin D binding protein: a multifunctional protein of clinical importance. *Adv Clin Chem*. 2014;63:1—57.
52. Bouillon R, Schuit F, Antonio L, et al. Vitamin D binding protein: a historic overview. *Front Endocrinol*. 2020;10:910.
53. McLeod JF, Cooke NE. The vitamin D-binding protein, alpha-fetoprotein, albumin multigene family: detection of transcripts in multiple tissues. *J Biol Chem*. 1989;264(36):21760—21769.

54. Dziegielewska KM, Saunders NR, Schejter EJ, et al. Synthesis of plasma proteins in fetal, adult, and neoplastic human brain tissue. *Dev Biol*. 1986;115(1):93—104.
55. Carlyle BC, Kitchen RR, Kanyo JE, et al. A multiregional proteomic survey of the postnatal human brain. *Nat Neurosci*. 2017;20(12):1787—1795.
56. Geiger T, Velic A, Macek B, et al. Initial quantitative proteomic map of 28 mouse tissues using the SILAC mouse. *Mol Cell Proteomics*. 2013;12(6):1709—1722.
57. Huttlin EL, Jedrychowski MP, Elias JE, et al. A tissue-specific atlas of mouse protein phosphorylation and expression. *Cell*. 2010;143(7):1174—1189.
58. Jirikowski GF, Kauntzer UW, El Emmam Dief A, et al. Distribution of vitamin D binding protein expressing neurons in the rat hypothalamus. *Histochem Cell Biol*. 2009;131(3):365—370.
59. Moon M, Song H, Hong HJ, et al. Vitamin D-binding protein interacts with Aβ and suppresses Aβ-mediated pathology. *Cell Death Differ*. 2013;20(4):630—638.
60. Jeon SG, Cha MY, Kim JI, et al. Vitamin D-binding protein-loaded PLGA nanoparticles suppress Alzheimer's disease-related pathology in 5XFAD mice. *Nanomed Nanotechnol Biol Med*. 2019;17:297—307.
61. Kułakowska A, Tarasiuk J, Kapica-Topczewska K, et al. Pathophysiological implications of actin-free Gc-globulin concentration changes in blood plasma and cerebrospinal fluid collected from patients with Alzheimer's disease and other neurological disorders. *Adv Clin Exp Med*. 2018;27(8):1075—1080.
62. Zhang J, Sokal I, Peskind ER, et al. CSF multianalyte profile distinguishes Alzheimer and Parkinson diseases. *Am J Clin Pathol*. 2008;129(4):526—529.
63. Xiao F, Chen D, Lu Y, et al. Proteomic analysis of cerebrospinal fluid from patients with idiopathic temporal lobe epilepsy. *Brain Res*. 2009;1255:180—189.
64. Sengupta N, Mukherjee S, Tripathi P, et al. Cerebrospinal fluid biomarkers of Japanese encephalitis. *F1000Research*. 2015;4:334.
65. Yang M, Qin Z, Zhu Y, et al. Vitamin D-binding protein in cerebrospinal fluid is associated with multiple sclerosis progression. *Mol Neurobiol*. 2013;47(3):946—956.
66. Perga S, Giuliano Albo A, Lis K, et al. Vitamin D binding protein isoforms and apolipoprotein E in cerebrospinal fluid as prognostic biomarkers of multiple sclerosis. *PLoS One*. 2015;10(6):e0129291.
67. Lee MY, Kim EY, Kim SH, et al. Discovery of serum protein biomarkers in drug-free patients with major depressive disorder. *Prog Neuro-Psychopharmacol Biol Psychiatry*. 2016;69:60—68.
68. Xu HB, Zhang RF, Luo D, et al. Comparative proteomic analysis of plasma from major depressive patients: identification of proteins associated with lipid metabolism and immunoregulation. *Int J Neuropsychopharmacol*. 2012;15(10):1413—1425.